

## Supplementary Information

# A new type of power energy for accelerating chemical reactions: the nature of a microwave-driving force for accelerating chemical reactions

Jicheng Zhou<sup>\*</sup>, Wentao Xu, Zhimin You, Zhe Wang, Yushang Luo, Lingfei Gao, Cheng Yin, Renjie Peng & Lixin Lan

Key Laboratory of Green Catalysis and Chemical Reaction Engineering of Hunan Province, School of Chemical Engineering, Xiangtan University, Xiangtan 411105, Hunan Province, China

**\*Corresponding author. Jicheng, Zhou; Tel.:+86-0731-58298173;**

**E-mail address: [zhoujicheng@sohu.com](mailto:zhoujicheng@sohu.com)**

## S1. Experimental section

### *S1.1 Preparation of the catalysts*

#### *S1.1.1 Preparation of the CuO-Cu-ZSM-5 catalyst*

Cu-ZSM-5 was prepared using the ion-exchange method. H-ZSM-5 (Si/Al=33 supplied by the Changling Petroleum Refining Catalyst Plant, China) was exchanged with an aqueous solution of 0.01 mol/L Cu(AC)<sub>2</sub> (AR grade, Shenyang Agent Company, China) according to a H-ZSM-5 to aqueous solution ratio of 15 g/L. Then, the solution was adjusted to a pH of 7 using ammonia followed by stirring for 12 h at 50 °C. After filtration, the sample was washed with deionized water, dried at 100 °C for 10 h and calcined at 500 °C

1 for 6 h. Ion exchange was performed 2 times to yield the final Cu-ZSM-5 zeolite catalyst  
2 containing 5 wt% of Cu.

3 The CuO-Cu-ZSM-5 catalyst was prepared using a mechanical mixing method. CuO  
4 was added to Cu-ZSM-5 and ground sufficiently and uniformly mixed in a mortar.

#### 5 *SI.1.2 Preparation of the BaMnO<sub>3</sub> and BaFeO<sub>3</sub> catalysts*

6 The BaBO<sub>3</sub> (B=Mn, Fe) mixed oxides were prepared using the sol-gel method.  
7 Ba(NO<sub>3</sub>)<sub>2</sub> (AR grade) and Mn(NO<sub>3</sub>)<sub>2</sub> (AR grade) or Fe(NO<sub>3</sub>)<sub>3</sub> (AR grade) were dissolved in  
8 deionized water according to a molar ratio of BaBO<sub>3</sub> (B=Mn, Fe). Citric acid and glycol  
9 were added to the aqueous solution, where the number of moles of the complexing species  
10 was 1.25 times that of the metal ions (i.e., Ba<sup>2+</sup> and Mn<sup>2+</sup> or Fe<sup>3+</sup>). The aqueous solutions  
11 were stirred at 80 °C for 2.5 h to obtain spongy amorphous gels. The acquired gels were  
12 dried at 120 °C overnight and submitted to decomposition in air at 400 °C for 2 h followed  
13 by calcination at 700 °C for 4 h.

#### 14 *SI.1.3 Preparation of AC*

15 Activated carbon (designated as AC, Φ3.0 mm, Sinopharm Chemical Reagent Co., Ltd.)  
16 was pretreated with an aqueous solutions consisting of HNO<sub>3</sub> (20 %) followed by drying at  
17 80 °C for 12 h.

#### 18 *SI.1.4 Preparation of the MeS/γ-Al<sub>2</sub>O<sub>3</sub>/BaMn<sub>0.2</sub>Cu<sub>0.8</sub>O<sub>3</sub> (Me=Ni, Co) catalysts*

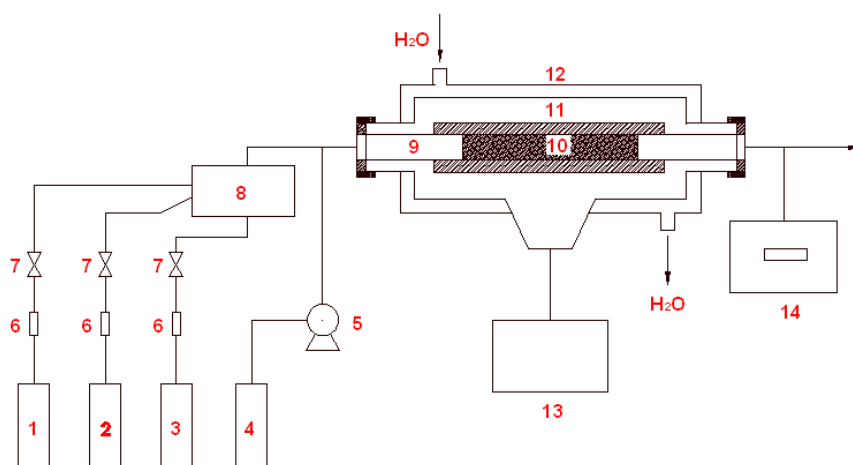
19 The NiS and CoS nanoparticles were prepared by the solvothermal method. The  
20 BaMn<sub>0.2</sub>Cu<sub>0.8</sub>O<sub>3</sub> samples were prepared with sol-gel method, and the acquired gels were  
21 dried at 120 °C overnight and submitted to decomposition in air at 400 °C for 2h and then  
22 calcined at 700 °C for 4 h.

1 The  $\text{MeS}/\gamma\text{-Al}_2\text{O}_3/\text{BaMn}_{0.2}\text{Cu}_{0.8}\text{O}_3$  (Me=Ni,Co) catalysts were prepared using a  
 2 mechanical mixing method. MeS (Me=Co, Ni) and  $\text{BaMn}_{0.2}\text{Cu}_{0.8}\text{O}_3$  (30 % by weight NiS  
 3 and 40 % by weight  $\text{BaMn}_{0.2}\text{Cu}_{0.8}\text{O}_3$ , or 30 % by weight CoS and 60 % by weight  
 4  $\text{BaMn}_{0.2}\text{Cu}_{0.8}\text{O}_3$ , respectively) were added to  $\gamma\text{-Al}_2\text{O}_3$  (surface area:  $200\text{ m}^2/\text{g}$ ), and the  
 5 mixture was ground and mixed uniformly in a mortar. Then, the powders were formed into  
 6 pellets by compression and sieved to 0.180-0.850 mm.

7

## 8 *S1.2 Activity evaluation*

### 9 *S1.2.1 Microwave reactor system*



10

11 **Figure S1** Schematic diagram of the microwave catalytic reactor system

12 1. NO; 2. O<sub>2</sub>; 3. N<sub>2</sub>; 4. Storage tank; 5. Metering pump; 6. Mass flow meter; 7. Valve; 8. Premixer; 9.  
 13 Quartz reactor; 10. Fixed bed; 11. Thermal insulation; 12. Resonant cavity; 13. Microwave generator; 14.  
 14 On-line NO<sub>x</sub> analyser.

15

16 A multi-mode microwave catalytic reactor system was applied to investigate the role of  
 17 microwave irradiation on a continuous flow of gas-solid catalytic reaction system. The  
 18 experimental diagram is shown in Fig. S1. The reactor consisted of a microwave generator

1 system and a reaction system. The microwave energy was supplied by a 2.45 GHz  
2 microwave generator, and the power could be adjusted continuously in a range of 0-1000 W.  
3 The magnetron microwave source was connected through a rectangular waveguide to a  
4 resonant cavity ( $\Phi 28$  mm\*320 mm, the space of microwave irradiation is not only the  
5 catalyst but the whole cavity). A quartz tube (i.d.10 mm and 540 mm in length) at the centre  
6 of the cavity was designed to accommodate the experiments. The catalyst was placed in the  
7 middle of the quartz tube, and both ends of the tube were sealed with asbestos. Reliable  
8 monitoring of the reaction temperature is nontrivial but absolutely critical to the  
9 investigation of the microwave effects. Therefore, the temperature of the reaction bed was  
10 provided by microwave thermal effect and precisely measured by a modified thermocouple  
11 probe, which was coated with a tin-aluminium alloy to shield the microwave irradiation of  
12 the modified thermocouple itself and inserted into the catalyst bed. The advantages of this  
13 microwave reactor system are as follows:

14 (1) Continuously adjustable microwave power in the range of 0-1000 W with a  
15 frequency of 2450 MHz.

16 (2) The temperature of the catalyst bed can be precisely controlled by a microcomputer.

17 (3) The temperature of the catalyst bed can be measured precisely.

18 (4) The microwave source emits microwaves and irradiates the reaction tube, and the  
19 circulating water system is surrounds the periphery of the furnace chamber to absorb the  
20 microwaves to avoid damage to the magnetron caused by the reflected microwaves, which  
21 could protect the magnetron and allow the microwave catalytic reaction to continue to run  
22 for a long period of time.

1 *SI.2.2 Activity tests*

2 For the direct catalytic decomposition of NO over the CuO-Cu-ZSM-5 catalysts, the  
3 reactant gas was composed of NO (molar fraction, 0.1%), O<sub>2</sub> (molar fraction, 5.88%) and N<sub>2</sub>  
4 as the balance gas. All of the prepared catalysts had a granule size of 300-700 μm. The flow  
5 rate of the feed was 160 ml min<sup>-1</sup> (GHSV = 1600 h<sup>-1</sup>, τ = 2.25 s).

6 For the direct catalytic decomposition of NO over the BaMnO<sub>3</sub> and BaFeO<sub>3</sub> catalysts,  
7 the catalysts (2.0 g, 20-60 mesh) were used for each run, and the reactant feed rates were  
8 fixed at W/F = 1 g s cm<sup>-3</sup>, where W and F are the catalyst weight and the total flow rate of  
9 reactant gas (F=120 ml min<sup>-1</sup>), respectively.

10 For the reduction of NO by AC, the reactant gas was composed of NO (molar fraction,  
11 0.1 %) and O<sub>2</sub> (molar fraction, 5.8 %) and N<sub>2</sub> as the balance gas. Ten millilitres of catalyst  
12 were used for each run, and the space velocity (GHSV) was 1020 h<sup>-1</sup>.

13 For comparison, the CRM and MCRM were carried out in the same size reactor with  
14 the same reaction bed amount under identical conditions. In the CRM, the reaction test was  
15 carried out using a microreactor device (MRT-6123; Beijing Xin Hang Shield Petrochemical  
16 Technology Co., Ltd.). The concentrations of NO and NO<sub>2</sub> in the outlet gas were analysed  
17 by an online NO<sub>x</sub> analyser (42C, Thermo Environmental Instruments Co., Ltd., U.S.). In  
18 addition, the analysis system consisted of GC (Agilent 7890A) with a thermal conductivity  
19 detector and a Porapak Q column for N<sub>2</sub>O analysis. In the MCRM, N<sub>2</sub> was the desired  
20 product, NO<sub>2</sub> was the by-product, and N<sub>2</sub>O was not detected. Therefore, the NO conversion  
21 and N<sub>2</sub> selectivity was calculated using the following formulas:

22 
$$X_{NO} = \frac{C_0(NO) - C_1(NO)}{C_0(NO)} \times 100\% \quad , \quad S_{NO} = \frac{C_0(NO) - C_1(NO) - C_1(NO_2)}{C_0(NO) - C_1(NO)} \times 100\%$$

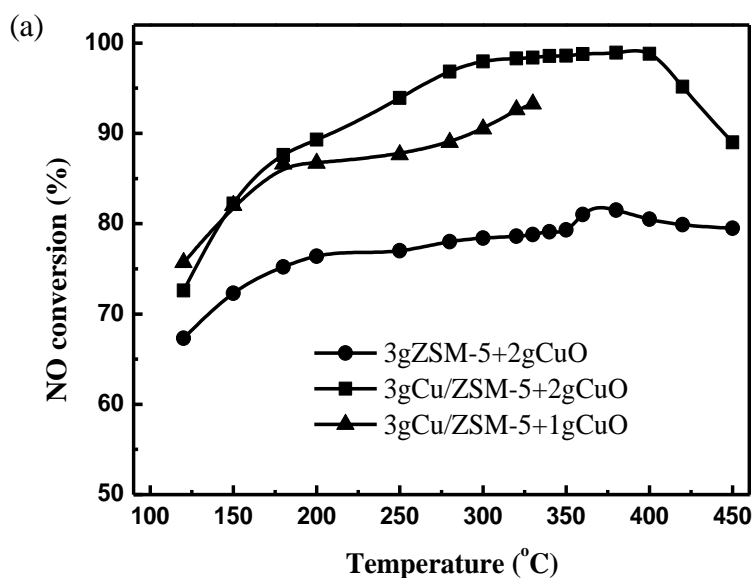
1  $(X_{NO}$  represents the NO conversion,  $S_{NO}$  represents the  $N_2$  selectivity,  $C_0(NO)$  represents the NO  
2 concentration prior to the reaction,  $C_1(NO)$  represents the NO concentration after the reaction, and  
3  $C_1(NO_2)$  represents the  $NO_2$  concentration after the reaction.)  
4

5 For the direct catalytic decomposition of NO over the  $BaMnO_3$  and  $BaFeO_3$  catalysts,  
6 the reactor contains a flow of feed gas (15 vol%  $H_2S$  in  $N_2$ , 60 ml/min) that passes through  
7 the quartz tube, and the hydrogen content was analysed using gas chromatography (Agilent  
8 GC 7890 A) with a thermal conductivity detector (TCD) and a Porapak Q column (80-100  
9 mesh, with 6ft\*1/8”\*2.0 mm). The operation temperature of the column was 80°C. A  
10 sample of the  $MeS/\gamma-Al_2O_3/BaMn_{0.2}Cu_{0.8}O_3$  catalyst (m=2 g) was transferred to the  
11 microwave catalytic reactor system. The system was initially purged with nitrogen gas to  
12 prevent air oxidation or moisture uptake. A continuous stream of  $N_2$ , was employed, and  
13 when the catalyst bed reached the required reaction temperature under microwave  
14 irradiation, the  $H_2S$  valve was opened. The exit gas was analysed by GC at four minute  
15 intervals until consistent results were obtained for each reaction condition. During  $H_2S$   
16 decomposition, only  $H_2$  and sulfur were produced without any other by-products. Therefore,  
17 the  $H_2$  yield directly reflects the efficiency of  $H_2S$  decomposition, and the selectivity to  
18 hydrogen was always 100%. In addition, the  $H_2S$  conversion can be expressed as follows:

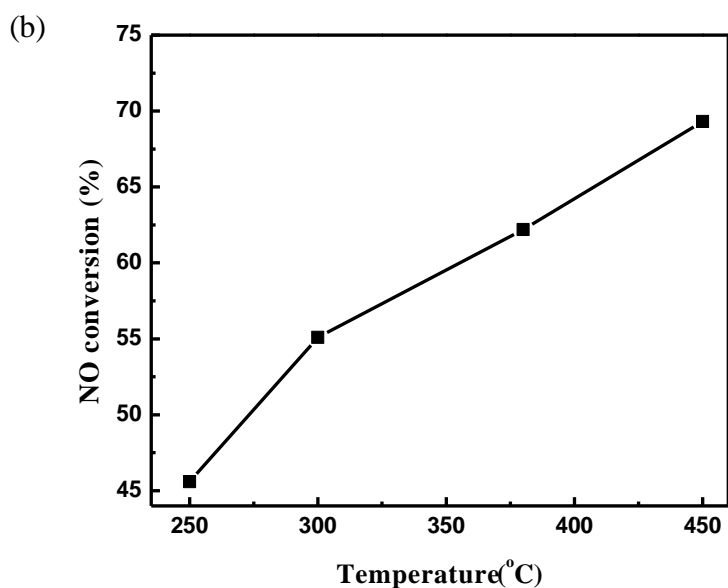
$$X_{H_2S} = \frac{Y_{H_2}}{V_{H_2S}^o} 100\%$$

19  
20 where  $X_{H_2S}$  is the  $H_2S$  conversion based on the formation of hydrogen.  $V_{H_2S}^o$  is the initial  
21 volume fraction of hydrogen sulfide (15 % here).  
22

1 **S2. Results and discussion**



2



3

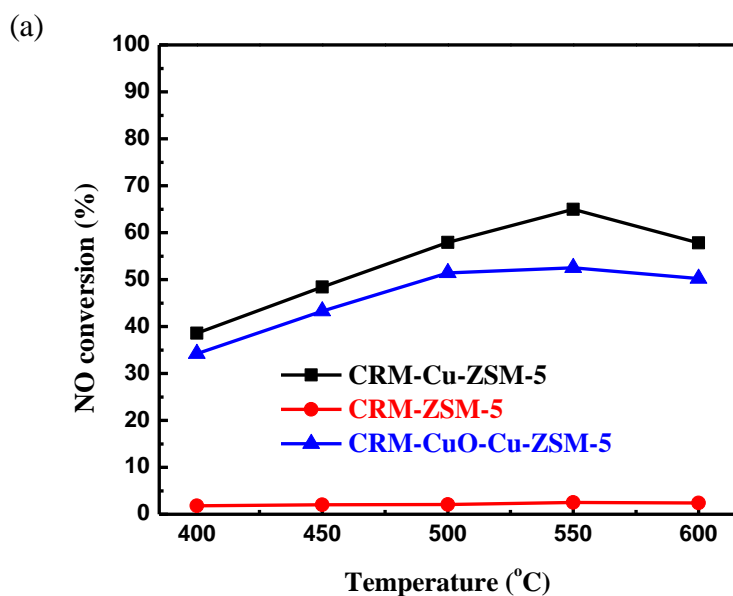
4 **Figure S2.** Effect of temperature on the direct decomposition of NO over 3 g Cu ZSM-5+2

5 g CuO (■), 3 g ZSM-5+2 g CuO (●), 3 g Cu ZSM-5+1 g CuO (▲) (a) and single 4 g CuO

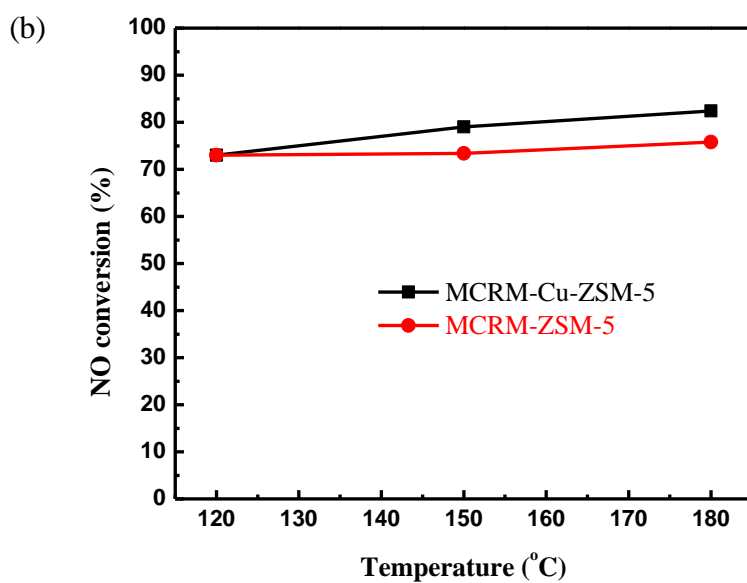
6 (b) in the MCRM. (Gas mixture: 1000 ppm NO, 5.88% O<sub>2</sub>, N<sub>2</sub> as a balancing gas, GHSV =

7 1600 h<sup>-1</sup>).

8



1



2

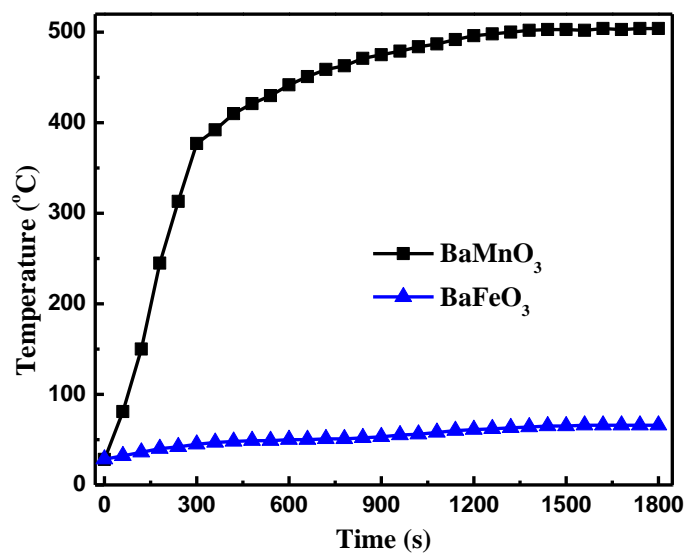
3 **Figure S3.** (a). Activity of NO conversion over 4 g ZSM-5, 4 g Cu-ZSM-5 and 3 g  
 4 Cu-ZSM-5+1 g CuO in the CRM. (Gas mixture: 1000 ppm NO, 5.88% O<sub>2</sub>, N<sub>2</sub> as a  
 5 balancing gas, GHSV = 1600 h<sup>-1</sup>).

6 (b). Activity of NO conversion over 4 g ZSM-5 and 4 g Cu-ZSM-5 in the MCRM.  
 7 (Gas mixture: 1000 ppm NO, 5.88% O<sub>2</sub>, N<sub>2</sub> as a balancing gas, GHSV = 1600 h<sup>-1</sup>)

8

9





1

2 **Figure S4.** Microwave heating behaviour of the BaMnO<sub>3</sub> and BaFeO<sub>3</sub> catalysts in the

3 MCRM using a microwave power of 150 W.

4

5

6

7

8

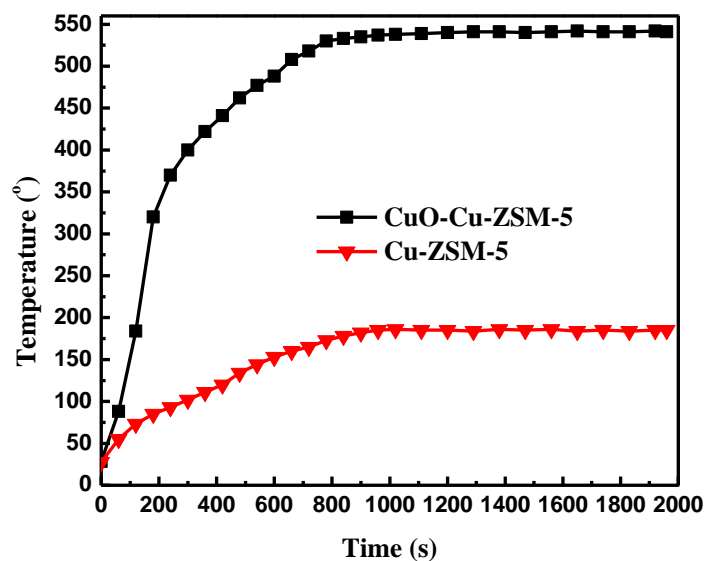
9

10

11

12

13



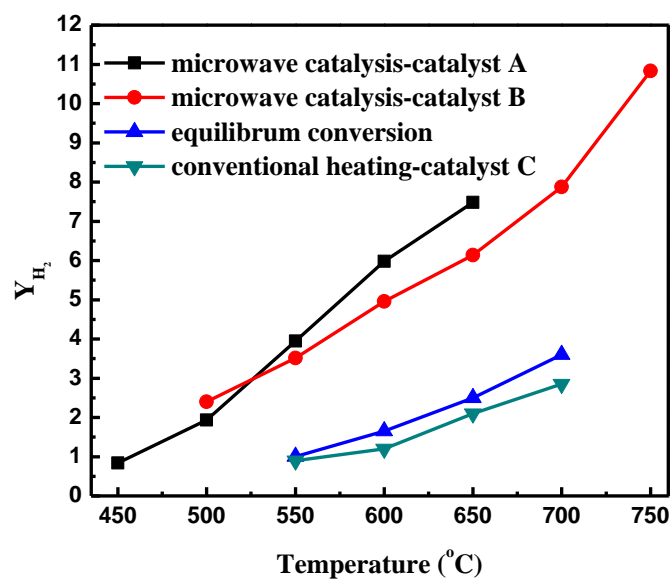
1

2 **Figure S5.** Microwave heating behaviour of CuO-Cu-ZSM-5 and single Cu-ZSM-5 in the  
 3 MCRM using a microwave power of 150 W.

4

5 As shown in Fig. S5, the stable temperature of the bed was maintained at only 185 °C  
 6 for single Cu-ZSM-5 under microwave irradiation for approximately 30 min at a microwave  
 7 power of 300 W. Comparatively, the stable temperature of the bed was maintained at 541 °C  
 8 for CuO-Cu-ZSM-5 at the same microwave power and irradiation time. The results indicate  
 9 that MW adsorption property of the CuO-Cu-ZSM-5 catalyst is stronger than that of the  
 10 single Cu-ZSM-5 catalyst.

11



1

2 **Figure S6.** H<sub>2</sub> yield as a function of temperature with microwave catalysis-catalyst A:

3 NiS/ $\gamma$ -Al<sub>2</sub>O<sub>3</sub>/BaMn<sub>0.2</sub>Cu<sub>0.8</sub>O<sub>3</sub>; microwave catalysis-catalyst B: CoS/ $\gamma$ -Al<sub>2</sub>O<sub>3</sub>/BaMn<sub>0.2</sub>Cu<sub>0.8</sub>O<sub>3</sub>;

4 and conventional heating-catalyst C: MoS<sub>2</sub>/ $\gamma$ -Al<sub>2</sub>O<sub>3</sub>.

5

6

7

8

9

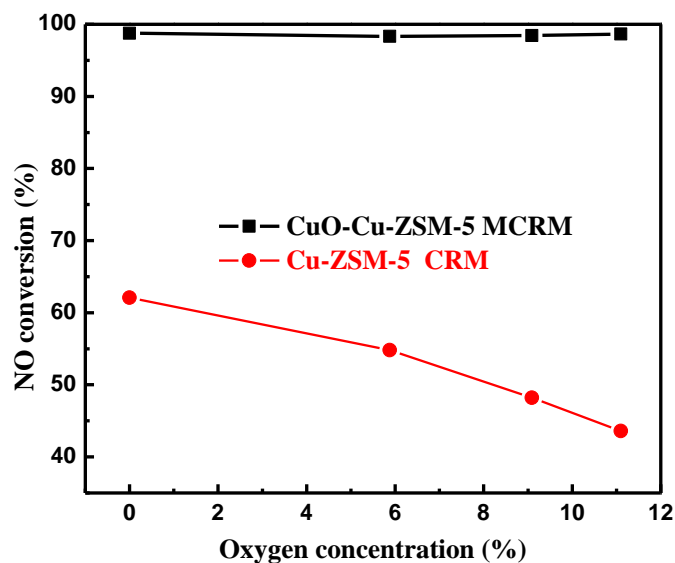
10

11

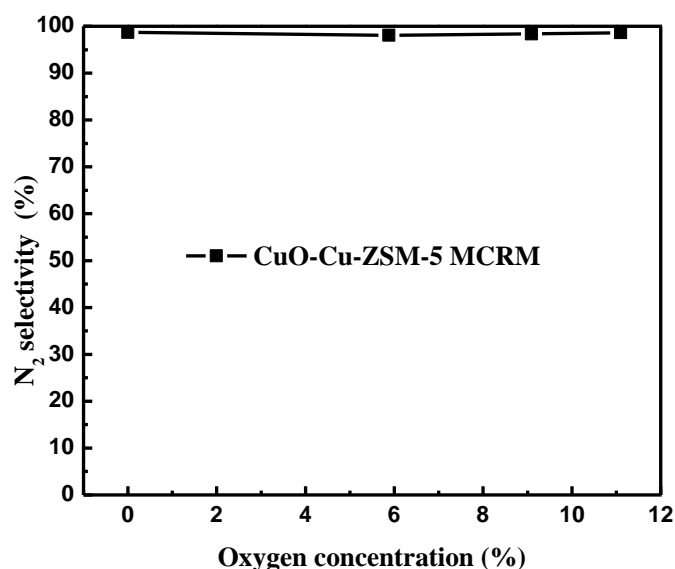
12

13

14



1



2

3 **Figure S7.** Effects of oxygen concentrations on NO conversion over CuO-Cu-ZSM-5 in the  
 4 MCRM and Cu-ZSM-5 in the CRM (a). Effects of O<sub>2</sub> concentrations on the N<sub>2</sub> selectivity  
 5 over CuO-Cu-ZSM-5 in the MCRM (b) (Reaction conditions: reaction temperature, 300 °C  
 6 in the MCRM and 550°C in the CRM, respectively; molar fraction of NO, 0.1%; N<sub>2</sub> as a  
 7 balancing gas; and ambient temperature, 32°C).

8

9 As shown in Fig. S7, the oxygen concentration does not influence the NO conversion or  
 10 N<sub>2</sub> selectivity over the CuO-Cu-ZSM-5 MW catalyst in the MCRM. However, the N<sub>2</sub>  
 11 conversion in the CRM decreased from 62.1% to 43.6% when the oxygen concentration

1 gradually increased from 0 % to 11.1 %. The CuO-Cu-ZSM-5 catalyst exhibited good  
2 stability to excessive oxygen in the MCRM even though Cu-ZSM-5 can be deactivated due  
3 to the adsorption of coexisting oxygen in the CRM. Moreover, the N<sub>2</sub> selectivity in the  
4 MCRM was more than 98.1 % (Fig. S7b). The high selectivity indicates that the undesirable  
5 consecutive reactions of NO with O<sub>2</sub> to generate NO<sub>2</sub> and NO conversion to N<sub>2</sub>O barely  
6 occurred in the MCRM, and nearly the entire NO was directly converted to N<sub>2</sub>. At the same  
7 time, we previously also found the NO conversion and N<sub>2</sub> selectivity were up to 99.8% and  
8 99.9%, respectively for BaMn<sub>0.9</sub>Mg<sub>0.1</sub>O<sub>3</sub> catalyst even with the coexistence of 10% oxygen  
9 and low temperature of 250 °C.<sup>[S1]</sup>

10 The oxygen concentration does not influence the catalytic performance of the  
11 CuO-Cu-ZSM-5 MW catalyst for NO decomposition in the MCRM. This phenomenon is in  
12 agreement with our previous results.<sup>[S1,S2]</sup> The microwave selective effect under microwave  
13 irradiation may account for this phenomenon. Polar molecules are most easily activated by a  
14 microwave electromagnetic field. As we previously reported<sup>[S1,S2]</sup>, the NO molecules that  
15 adsorbed on the active sites rather than O<sub>2</sub> molecules in the gas phase can be activated  
16 effectively by the microwave electromagnetic field. Although both O<sub>2</sub> and NO molecules  
17 can be physically adsorbed on the active sites, only physically adsorbed NO molecules in  
18 the MCRM become chemically adsorbed and further converted to N<sub>2</sub> and O<sub>2</sub>.  
19 Simultaneously, O<sub>2</sub> molecules cannot be activated at this low reaction temperature due to  
20 the microwave selective effect, and they cannot react with NO molecules to form NO<sub>2</sub>.  
21 Therefore, the CuO-Cu-ZSM-5 MW catalyst in the MCRM exhibited outstanding stability  
22 to excess oxygen.

1 **Table S1** Apparent activation energies (Ea') of NO reduction by AC.

Mode/Temperature conditions	Ea' (kJ/mol)
CRM, 250-300 °C	29.853
MCRM, 250-300 °C	19.718

2

3

4

5

6

7

8

9

10

11 **Table S2** Apparent activation energies (Ea') of direct catalytic decomposition of H<sub>2</sub>S.

Mode/Temperature conditions	Catalysts	Ea' (kJ/mol) <sup>a</sup>	Reference
MCRM, 450-650 °C	NiS/ $\gamma$ -Al <sub>2</sub> O <sub>3</sub> /BaMn <sub>0.2</sub> Cu <sub>0.8</sub> O <sub>3</sub>	26.83	This work
MCRM, 650-750 °C	CoS/ $\gamma$ -Al <sub>2</sub> O <sub>3</sub> /BaMn <sub>0.2</sub> Cu <sub>0.8</sub> O <sub>3</sub>	19.46	This work
CRM, 650-850 °C	NiS,MoS <sub>2</sub>	69.04	S4
CRM, 650-850 °C	CoS,MoS <sub>2</sub>	59.21	S4
CRM, 500-900 °C	$\gamma$ -Al <sub>2</sub> O <sub>3</sub>	72	S5
CRM, 600-800 °C	No catalyst	495.62	S6

12 <sup>a</sup>Ea' were calculated using the Arrhenius equation; Kinetic data was calculated according to ref.[S3].

13

14

15

16

17

18

1 **Table S3** Effect of microwave input power on the balanced bed temperature over the  
 2 CuO-Cu-ZSM-5 and single Cu-ZSM-5 catalysts.

Microwave power (W)	CuO-Cu-ZSM-5 Balanced bed T (°C)	Cu-ZSM-5 Balanced bed T (°C)
400	299	196
600	367	225
800	412	242
1000	450	261

3

4

5

6

7

8

9

10

11 **Table S4** Effect of the microwave input power on the balanced bed temperature over the  
 12 BaMnO<sub>3</sub> and BaFeO<sub>3</sub> catalysts.

Microwave power (W)	BaMnO <sub>3</sub> Balanced bed T (°C)	BaFeO <sub>3</sub> Balanced bed T (°C)
50	259	37
100	426	49
150	503	66

13

14

15

16

1 **Table S5** Effect of the microwave input power on the balanced bed temperature over AC.

Microwave power (W)	Balanced bed T (°C)
200	141
250	179
300	206
350	259
400	304

2

3

4

5

6

7

8

9

10 **Table S6** Effect of the microwave input power on the balanced bed temperature over the  
 11 MeS/ $\gamma$ -Al<sub>2</sub>O<sub>3</sub>/BaMn<sub>0.2</sub>Cu<sub>0.8</sub>O<sub>3</sub> (Me=Ni, Co) catalysts.

Microwave power (W)	NiS/ $\gamma$ -Al <sub>2</sub> O <sub>3</sub> /BaMn <sub>0.2</sub> Cu <sub>0.8</sub> O <sub>3</sub>	CoS/ $\gamma$ -Al <sub>2</sub> O <sub>3</sub> /BaMn <sub>0.2</sub> Cu <sub>0.8</sub> O <sub>3</sub>
	Balanced bed T (°C)	Balanced bed T (°C)
400	520	682
600	581	730
800	624	788

12

13

14



1 **Table S7** Effect of the reaction temperature range on the  $E_a$  and pre-exponential factor (A)  
2 over the CuO-Cu-ZSM-5 catalyst.

reaction temperature range (°C)	$E_a$ (kJ.mol <sup>-1</sup> )	A (L.mol <sup>-1</sup> .h <sup>-1</sup> )
120-150	25.727	6.2336
150-180	22.468	47.284
180-200	14.790	119
200-250	25.378	8.167
250-280	54.542	0.01
280-300	59.652	0.0033
300-320	26.877	3.210
320-330	18.117	18.970
330-340	35.203	0.628
340-360	26.024	3.802
360-380	22.810	7.00
380-400	19.545	15.839

3

4

5

## 6 **S section I**

7 In fact, MW irradiation involves polarization, which is different from conventional  
8 heating and leads to the changes of in the internal energy level of molecules to achieve  
9 activation. One portion of the MW energy was adsorbed by molecules, and another portion  
10 of the MW energy was released by the MW thermal effect. Upon microwave irradiation of  
11 gas-solid phase or liquid-solid phase reactions in the presence of MW catalysts, the  
12 microwaves interact with molecules of the MW catalysts and simultaneously with molecules

1 that participate in the reactions. For other reaction systems, such as liquid-liquid phase  
2 reactions and solid-phase reactions, microwaves directly interact with molecules that  
3 participate in the reaction under MW irradiation.

4 The results indicate that the different MW adsorption properties of catalysts with the  
5 same catalytic active component exhibit different catalytic performances under MW  
6 irradiation. Therefore, K was dependent on the dielectric properties of materials or MW  
7 catalysts under MW irradiation.

$$8 \quad E_{a_{MW}} = \frac{kE_{MW}P_{MW}}{1 + kE_{MW}P_{MW}} E_t \quad (9)$$

9  $E_{a_{MW}}$  can be calculated using Eq. (9). The decrease in the  $E_a$ ' can be calculated using  
10 Eq. (10).

11 where  $E_{a_0}$  is the activation energy barrier of the chemical reactions without MW irradiation.  
12 K is determined by the dielectric properties of the materials or MW catalysts as well as the  
13 MW frequency.

14

## 15 **S section II**

### 16 **Explanation and elucidate about experiment phenomenon and reaction results under** 17 **MW irradiation**

18 \*1 MW irradiation on chemical reactions can significantly reduce the  $E_a$ ' to activate  
19 reactant molecules and simultaneously increase the pre-exponential factor (A), which leads  
20 to substantially speeded up chemical reaction rates that increase the reaction conversion or  
21 shorten the reaction time.

22 \*2 MW irradiation of a chemical reaction can substantially reduce the  $E_a$ ' to activate  
23 reactant molecules and simultaneously increase the pre-exponential factor (A). Therefore,

1 the reactions can be achieved under mild conditions compared to those of conventional  
2 heating. The reaction temperature decreased by as much as several hundreds of degrees  
3 centigrade under MW irradiation, and some reactions that do not proceed using  
4 conventional heating are successfully performed under MW irradiation. For the same reason,  
5 the reduction in the  $E_a$ ' of reactions may result in these reactions occurring under mild  
6 conditions. Therefore, the temperature of solid-phase chemical reaction systems is  
7 substantially lower under MW irradiation. For example, the temperature of solid calcination  
8 reactions or crystalline phase reactions was reduced by 100-300 °C.

9 \*3 MW irradiation interacts with matter or/and catalysts in chemical reaction systems,  
10 which resulted in a selective effect due to the difference in the interactions between the MW  
11 irradiation and matter. Therefore, the selective effect of MW irradiation resulted in an  
12 increase in the yield or change in the product distribution. This result is different from that  
13 obtained using conventional heating, where heat transfer does not produce a selective effect  
14 in the stationary state. For the same reason, the selective effect of MW irradiation results in  
15 an increase in the yield or change in the crystalline purity of solid-phase or liquid-solid  
16 phase reaction systems<sup>S7</sup>.

17 \*4 MW irradiation interacts with matter or/and catalysts in chemical reaction systems,  
18 which resulted in a selective effect. The selective effect of MW irradiation may cause the  
19 difference in speeding up forward and reverse reactions for reversible chemical reactions.  
20 Therefore, this result is very different from that of a catalyst using conventional heating that  
21 typically speeds up the forward and reverse reactions, which results in no selective effect.  
22 Therefore, the MW selective effect can increase the equilibrium conversion for a reversible

1 chemical reaction. For example, the equilibrium conversion of H<sub>2</sub> for the direct H<sub>2</sub>S  
2 decomposition reaction increases from 5 % up to 11.2 % at same reaction temperature of  
3 750 °C (Fig. S6) and from 6 % to 20 % at same reaction temperature of 800 °C<sup>S8</sup>. Therefore,  
4 the MW selective effect disrupts the restriction of the reaction equilibrium conversion.

5 In our previous study<sup>S7-S8</sup>, we reported that the MW selective effect for the microwave  
6 direct catalytic decomposition of NO resulted in no oxygen inhibition for competition  
7 reactions. Microwaves interact with polar molecules rather than with non-polar molecules,  
8 and microwave irradiation is beneficial for the activation of polar molecules. NO and O<sub>2</sub>  
9 molecules can be physically adsorbed on the active sites. However, only the physically  
10 adsorbed NO molecules became chemically adsorbed on the active sites and were further  
11 converted to N<sub>2</sub> in the MCRM. The physical adsorption of O<sub>2</sub> molecules is not enough to be  
12 activated at low temperatures under microwave irradiation, and the molecules do not react  
13 with NO to generate NO<sub>2</sub>. These results indicated the elimination of oxygen inhibition for  
14 the direct decomposition of NO over the BaMn<sub>1-x</sub>Mg<sub>x</sub>O<sub>3</sub> catalysts in the MCRM<sup>S7</sup>.  
15 Therefore, microwave irradiation of the chemical reactions exhibited a microwave-selective  
16 effect.

17

18

19

### 20 **S3. References:**

21 S1 Xu, W., Zhou, J., Ou, Y., Luo, Y. & You, Z. Microwave selective effect: a new approach  
22 towards oxygen inhibition removal for highly-effective NO decomposition by  
23 Microwave catalysis over BaMn<sub>x</sub>Mg<sub>1-x</sub>O<sub>3</sub> mixed oxides at low temperature under excess

- 1 oxygen. *Chem. Comm.* 51, 4073-4076 (2015).
- 2 S2 Xu, W., Zhou, J., You, Z., Luo, Y. & Ou, Y. Microwave Irradiation Coupled with  
3 Physically Mixed MeO (Me=Mn,Ni) and Cu-ZSM-5 Catalysts for the Direct  
4 Decomposition of Nitric Oxide under Excess Oxygen. *ChemCatChem* 7, 450-458  
5 (2015).
- 6 S3 Reshetenko, T., Khairulin, S., Ismagilov, Z. & Kuznetsov, V. Study of the reaction of  
7 high-temperature H<sub>2</sub>S decomposition on metal oxides ( $\gamma$ -Al<sub>2</sub>O<sub>3</sub>, $\alpha$ -Fe<sub>2</sub>O<sub>3</sub>,V<sub>2</sub>O<sub>5</sub>). *Int. J.*  
8 *Hydrogen Energy* 27, 387-394 (2002).
- 9 S4 Yumura, M. & Furimsky, E. Hydrogen sulphide adsorption and decomposition in the  
10 presence of manganese nodules. *Appl. Catalysis* 16, 157-167 (1985).
- 11 S5 Al-Shamma, L. & Naman, S. The production and separation of hydrogen and sulfur from  
12 thermal decomposition of hydrogen sulfide over vanadium oxide/sulfide catalysts. *Int. J.*  
13 *Hydrogen Energy* 15, 1-5 (1990).
- 14 S6 Kaloidas, V.E. & Papayannakos, N.G Kinetic studies on the catalyticdecompostion of  
15 hydrogen sulfide in a tubular reactor. *Ind. Eng. Chem. Res.* 30, 345-351 (1991).
- 16 S7 Panda, A.B., Glaspell, G & El-Shall, M.S. Microwave synthesis of highly aligned ultra  
17 narrow semiconductor rods and wires. *J. Am. Chem. Soc.* 128, 2790-2791 (2006).
- 18 S8 Zhang, X. & Hayward, D.O. Applications of microwave dielectric heating in  
19 environment-related heterogeneous gas-phase catalytic systems. *Inorg. Chim. Acta* 359,  
20 3421-3433 (2006).